Hindawi Publishing Corporation
Journal of Nanomaterials
Volume 2011, Article ID 142463, 7 pages
doi:10.1155/2011/142463

Research Article

Effect of Applied Potential on the Formation of Self-Organized TiO_2 Nanotube Arrays and Its Photoelectrochemical Response

Chin Wei Lai and Srimala Sreekantan

School of Materials and Mineral Resources Engineering, Universiti Sains Malaysia Engineering Campus, Seberang Perai Selatan, Pulau Pinang, 14300 Nibong Tebal, Malaysia

Correspondence should be addressed to Srimala Sreekantan, srimala@eng.usm.my

Received 13 July 2011; Accepted 11 August 2011

Academic Editor: Renzhi Ma

Self-organized TiO_2 nanotube arrays have been fabricated by anodization of Ti foil in an electrochemical bath consisting of 1 M of glycerol with 0.5 wt% of NH_4F. The effects of applied potential on the resulting nanotubes were illustrated. Among all of the applied potentials, 30 V resulted in the highest uniformity and aspect ratio TiO_2 nanotube arrays with the tube's length approximately 1 μm and pore's size of 85 nm. TiO_2 nanotube arrays were amorphous in as-anodized condition. The anatase phase was observed after annealing at 400°C in air atmosphere. The effect of crystallization and effective surface area of TiO_2 nanotube arrays in connection with the photoelectrochemical response was reported. Photoelectrochemical response under illumination was enhanced by using the annealed TiO_2 nanotube arrays which have larger effective surface area to promote more photoinduced electrons.

1. Introduction

Since titanium oxide (TiO_2) is a commercial product in the early twentieth century, it is believed to be the most promising photocatalyst, due to its great capacity for oxidation, wide band gap, nontoxicity, low-cost, widespread availability, and long term stability [1–5]. Due to its wide range of functions, TiO_2 photocatalyst can be applied to the field of environmental cleanup including deodorization, antibacterial protection, antifouling protection, water treatment, emission gas treatment, dye-sensitized solar cells, hydrogen generation by water photoelectrolysis, gas sensors, and so on [4–8]. These applications can be roughly divided into "environmental" and "energy" categories. In this context, simple anodization method has caught the attention of the scientific community because vertically oriented and highly ordered TiO_2 nanotube arrays can be produced via this method [2, 9–12].

Heterogeneous photocatalysis is a well-known process in which a combination of photochemistry and catalysis are operating together [5, 13]. It implies that both light and catalyst are necessary to bring out the chemical reaction. Upon absorption of photons with energy larger than the band gap of TiO_2, electrons are excited from the valence band to the conduction band, creating electron-hole pairs [4, 13–15]. The valence band holes are powerful oxidants (+1 to +3.5 V versus NHE depending on the semiconductor and pH), while the conduction band electrons are good reductants (+0.5 to −1.5 V versus NHE). During photocatalytic hydrogen production, an essential photogeneration of electron-hole pairs is required. When photocatalysis is applied to perform water splitting process for hydrogen production, the reducing conduction band electrons become important as their role is to reduce protons to hydrogen molecules [14, 16–18].

The photocatalytic hydrogen production of TiO_2 is largely controlled by (i) the light absorption properties, (ii) reduction and oxidation rates on the surface by the electron and hole, and (iii) the electron-hole recombination rate [14, 19]. However, the main barriers of these activities are the rapid recombination of photogenerated electron-hole pairs as well as the backward reaction and the poor activation of TiO_2 by visible light [15, 20]. Shifting the threshold of its photoresponse into the visible region would definitely enhance its potential for solar energy conversion [14, 21].

In response to these problems, continuous efforts have been made to fabricate a highly efficient photocatalyst with a suitable architecture that could minimize the recombination of photogenerated electron-hole pairs. Therefore, in this paper, a detailed study has been performed to evaluate the morphology of the anodized Ti foil in different applied potential. The one-dimensional (1D) structure of nanotube arrays provides a high surface-to-volume ratio and excellent charge transfer properties if the precise design and control of the geometrical features are determined [21–24]. Such a mechanistic understanding is very important for the controlled growth of ordered TiO_2 nanotube structure that finds potential use in the development of viable hydrogen fuel cell for sustainable energy system.

2. Experimental

TiO_2 nanotube arrays were grown by anodic oxidation of titanium foils (4 cm × 1 cm) with 99.6% purity and 0.127 mm in thickness. Prior to anodization, the Ti foils were degreased by sonication in ethanol for 30 min. The foils were then rinsed in deionized water and dried with nitrogen stream. The anodization was performed in a two-electrode configuration bath with the Ti foil as the anode and the platinum rod as the counterelectrode. The electrolyte was homogenized via magnetic stirring. An experiment was done by adapting optimum condition for TiO_2 nanotubes formation, that is, anodization of Ti foil is performed at the feed rate of 0.1 V/sec, and the electrolyte is 0.5 wt% of NH_4F in 1 M of glycerol (85% glycerol and 15% water) for 30 minutes. The applied potential was varied from 10 to 50 V. The anodized Ti foils were cleaned using acetone and dried in nitrogen stream. After the cleaning and drying treatments, the as-anodized samples were annealed at 400°C for 2 hours in air atmosphere to convert to the TiO_2 anatase phase.

The morphology of the anodized Ti foils was viewed using a field emission scanning electron microscope (FESEM) Zeiss SUPRA 35 VP at a working distance of around 1 mm. In order to obtain the thickness of the anodic oxide formed, cross-sectional measurements were carried out on mechanically bent samples, where a partial liftoff of the anodic layer occurred. On top of that, the elemental analysis, that is, atomic percentage of the TiO_2, can be determined with EDX (energy dispersion X-ray) which is equipped in the FESEM. Phase determination of the anodic layer was determined by an X-ray diffraction (XRD) using Philips, PW 1729, operated at 45 kV and 40 mV.

The photoelectrochemical response of the samples were characterized using a three-electrode photoelectrochemical cell with TiO_2 nanotube arrays as the working photoelectrode, platinum rod as the counterelectrode, and saturated calomel electrode (SCE) was used as the reference electrode. 1 M KOH with 1 wt% of ethylene glycol solution was used as the electrolyte in this experiment. All of the three electrodes were connected to a potentiostat (μAutolab III). A Xenon lamp with an intensity of 800 W/m^2 (Zolix LSP-X150) was used to produce a largely continuous and uniform spectrum, and 100% transmittance of the light was permitted by the quartz glass as the xenon lamp shined on the TiO_2 nanotube arrays (photoanode). The Xenon lamp was switched on after the three electrodes were connected to the potentiostat. Then, a linear sweep potentiometry (LSP) was swept from −0.5 V to 1.0 V at a scan rate of 5 mV/s. During the voltage sweeping, the corresponding photocurrent was measured.

3. Results and Discussion

3.1. Surface Morphology of TiO_2 Nanotube Arrays. In this part of the experiment, the effect of applied potential on the morphology of the TiO_2 nanotube arrays is discussed. The formation of TiO_2 nanotube arrays in fluorinated electrolyte was the result of three simultaneously occurring processes: (1) field-assisted oxidation of Ti metal to form TiO_2, (2) field-assisted dissolution of Ti metal ions into electrolyte, and (3) chemical dissolution of Ti and TiO_2 in the presence of H^+ and F^- ions. In general, it can be concluded that the electrochemical condition is an important factor for the formation of well-aligned TiO_2 nanotube arrays [25, 26].

Figure 1 shows the FESEM images of surface morphology of the anodized Ti foils in electrolyte composed of 1 M of glycerol with 0.5 wt% of dissolved NH_4F for 30 minutes, and potential was varied from 10 V to 50 V. Insets are the cross-section morphology of the oxides. From these images, the appearance of the anodic oxides on the Ti foils was dependent on the applied potential in the fluorinated electrolyte. At low anodizing potential (10 V), pits started to form on the TiO_2 surface (Figure 1(a)). Upon increasing the potential to 20 V, 30 V, and 40 V, well-aligned TiO_2 nanotubes were observed (Figures 1(b)–1(d)). It is also apparent that the diameter of the pores increased from 50 nm to 110 nm when potential was raised from 20 V to 40 V. At 50 V, the intertubes' spacing was filled, and discrete nanotubes became more interconnected to form a nanoporous-like structure (Figure 1(e)). The average diameter, length, and surface area of the tube anodized at different applied potential are summarized in Table 1.

The diameter of the tubes was found to increase with the applied potential. The main reason may be attributed to the severe electric field dissolution which accelerates the formation of pits during the early stage of anodization. These pits were etched to form larger pore in higher potential. In addition, the increase in nanotube's length is attributed to the increased driving force for ionic species (H^+, F^-, and O^{2-}) to transport through the barrier layer at the bottom of the nanotube under electric field, which results in faster movement of the Ti/TiO_2 interface into the Ti metal. This improves the pore deepening and results in longer nanotube length. With the increase of applied potential, the rate of the fluoride (F^-) ions and the chemical dissolution at the barrier layer inside the nanotubes were increased, hence, allowing more oxygen (O^{2-}) to enter and oxidize the underlying Ti. This condition disrupts the self-ordering of nanotubular structure due to the imbalance reaction between the chemical dissolution, electric field dissolution, and oxidation process [7, 27, 28]. Besides, the anodic layer induces polarization of the Ti–O bond under higher applied potential and, hence, destroying the nanotubular structure. As a result, shorter

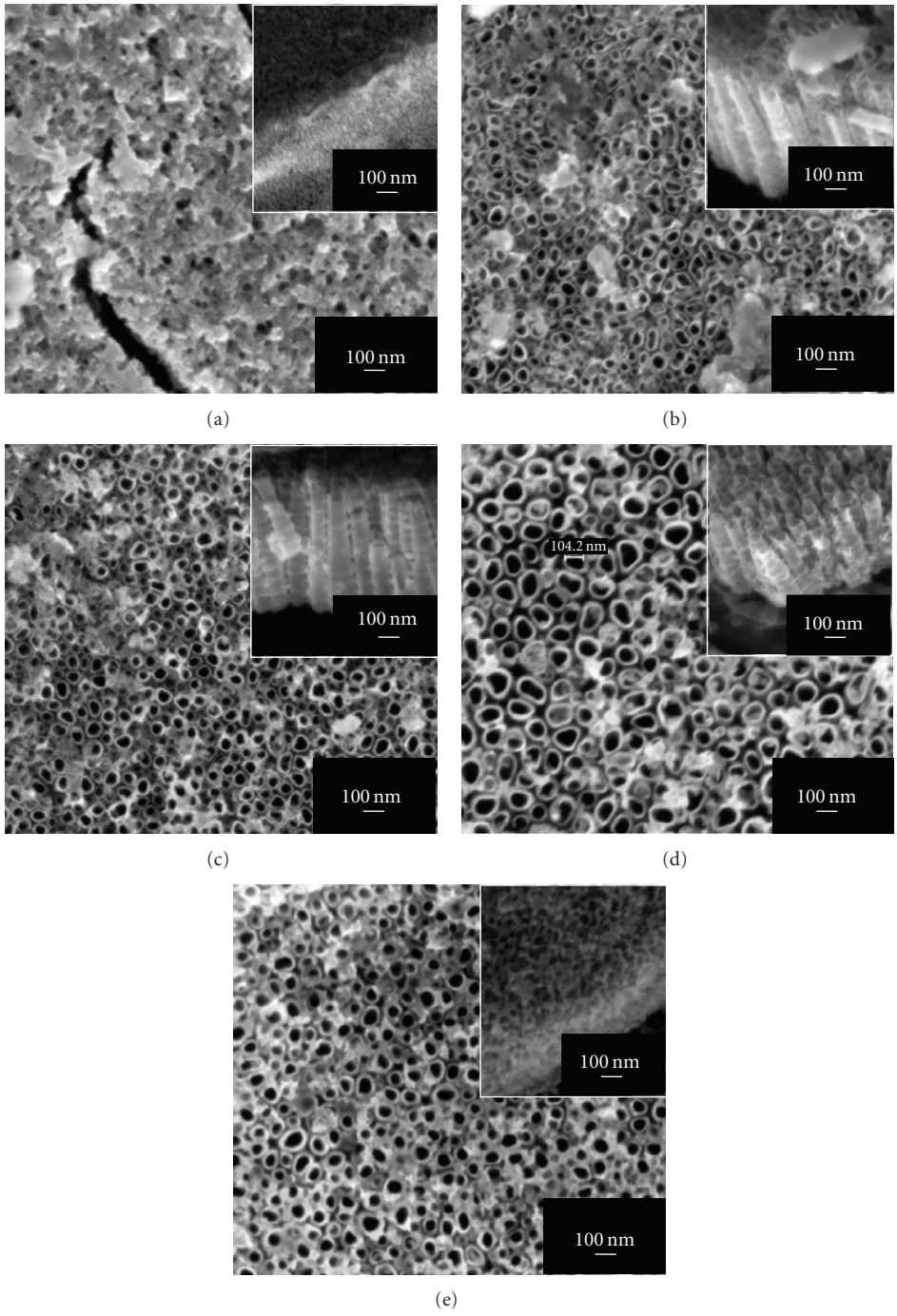

Figure 1: FESEM images of TiO_2 nanotube arrays fabricated at different applied potential in 1 M of glycerol electrolyte containing 0.5 wt% NH_4F for 30 minutes at (a) 10 V, (b) 20 V, (c) 30 V, (d) 40 V, and (e) 50 V. Insets are the cross-section morphology of the TiO_2 nanotube arrays.

length of irregular nanotubular structure was observed at higher applied potential. The dimensions and uniformity of the morphology of TiO_2 nanotube arrays were a function of applied potential in anodization process. Based on this study, 30 V was found to be the optimum potential for the formation of uniform circular nanotubes with lengths approaching 1 μm.

3.2. Formation Mechanism of TiO_2 Nanotube Arrays. In order to obtain the electrochemical information during the formation of TiO_2 nanotube arrays, a curve of current density versus time transient was plotted. Figure 2(a) shows the current density versus time curve recorded during anodization of Ti in 1 M of glycerol electrolyte containing 0.5 wt% NH_4F with a sweep rate of 0.1 V/s to 30 V for 30

Table 1: Dimension of the TiO_2 nanotube arrays anodized at different applied potential.

Potential (V)	Surface morphology	Length (nm)	Diameter (nm)	Average aspect ratio (L/D)
10	Nanoporous	275	—	—
20	Nonuniform nanotubes	750	Smaller tube = 50 Larger tube = 100	10
30	Uniform nanotubes	1000	~85	11.8
40	Nonuniform nanotubes	550	Smaller tube = 70 Larger tube = 110	6.1
50	Nonuniform nanotubes	250	Smaller tube = 40 Larger tube = 100	4.2

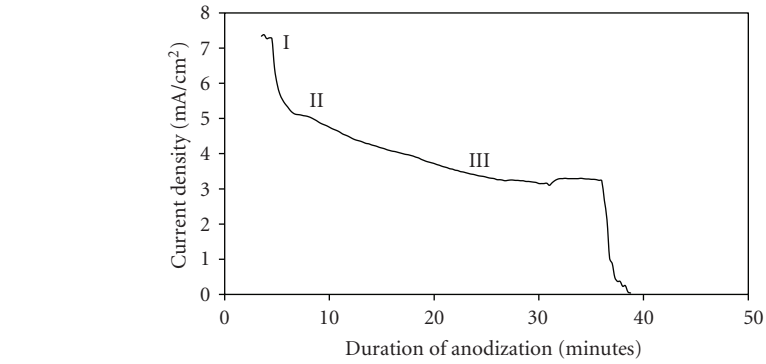

(a)

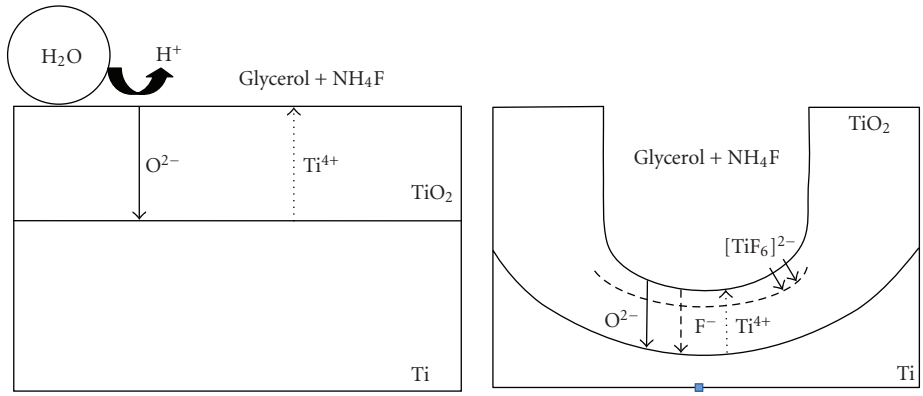

(b) (c)

Figure 2: (a) Current density against time plot for anodized Ti foils at 30 V for 30 minutes in 1 M glycerol electrolyte containing 0.5 wt% NH_4F, (b) schematic illustration to explain the formation of oxide layer (region I), and (c) schematic illustration to explain the dissolution of the barrier layer (region II).

minutes. Such plot is important to explain the mechanism of TiO_2 nanotube formation. Initially, there is an abrupt decrease of current as compact oxide layer is formed, which induces the potential drop between the Ti foil and the electrolytes. The existence of 15 wt% of water in the glycerol will contribute O^{2-} ions. The migration of O^{2-} ions towards the Ti/TiO_2 interface induces further growth of the barrier layer. This is the passivation process of Ti (region I), and a schematic illustration leading to the oxide layer formation is shown in Figure 2(b). The reaction occurred is depicted in the following equation:

$$Ti^{2+} + 2H_2O \longrightarrow TiO_2 + 4H^+ \quad (1)$$

In the second stage (region II), a slight increase in current was observed. As mentioned previously, high electric field across the thin layer will induce electric field dissolution. This is accompanied by breakdown of the passivated layer. Random pits are formed on the surface of the oxide due to polarization of Ti–O bond assisted by electric field across the sample. These random pits will grow into pores of various sizes and depths as the pits react with F^- ions to produce $[TiF_6]^{2-}$ complex ions as shown in (2). The chemical etching would slightly increase the current density as marked in region II. A schematic illustration regarding the dissolution of the barrier layer is exhibited in Figure 2(c) as follows:

$$TiO_2 + 4H^+ + 6F^- \longrightarrow [TiF_6]^{2-} + 2H_2O \quad (2)$$

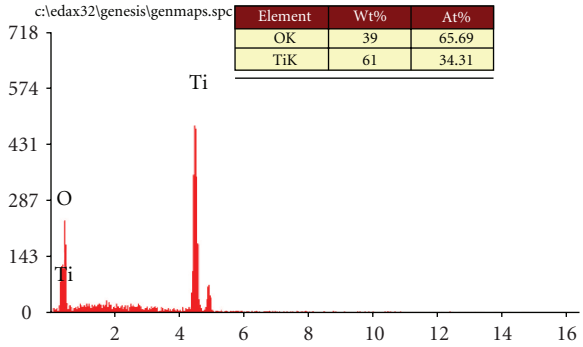

Figure 3: EDX spectra of TiO_2 nanotube arrays formed in glycerol electrolyte containing 0.5 wt% NH_4F at 30 V for 30 minutes.

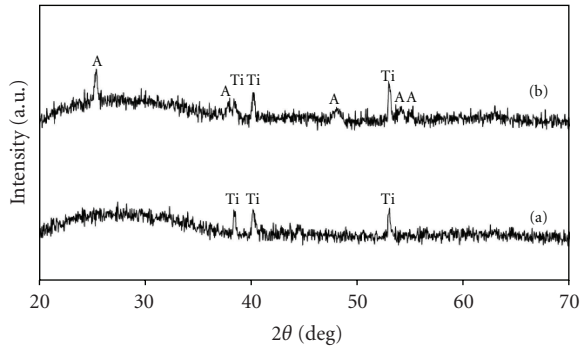

Figure 4: X-ray diffraction pattern of TiO_2 nanotubes (a) as anodized and (b) annealed at 400°C in air atmosphere for the sample formed in 1 M of glycerol electrolyte containing 0.5 wt% NH_4F at 30 V for 30 minutes (Ti = Titanium; A = Anatase).

In the third stage (region III), constant equilibrium was maintained with increasing anodization time whilst current density slightly reduced due to the change in pore's depth of the pits. The growth of pores is due to the competition between electrochemical oxide formation and chemical dissolution by F^- ions. Thus, the nanotube structure will grow inwards [27].

3.3. EDX Analysis of the Anodized TiO_2 Nanotube Arrays. The energy dispersive X-ray analysis (EDX) was employed to investigate the chemical stoichiometry of the Ti anodized and subsequently annealed at 400°C under the air atmosphere. From Figure 3, it can be concluded that the atomic ratio of Ti to O was approximately 1 : 2, indicating that only Ti and O elements were present without any impurities.

3.4. XRD Analysis of the Anodized TiO_2 Nanotube Arrays. It is well known that surface morphology change is closely related to crystal growth and phase transition. Therefore, XRD was used to investigate the effect of crystal growth and phase transition on the change in surface morphology of the TiO_2 nanotube arrays. Figure 4 depicts the XRD patterns of as-anodized and annealed TiO_2 nanotubes fabricated at 30 V in glycerol containing 0.5 wt% NH_4F. The presence of Ti phase was detected in the as-anodized sample, which represents the amorphous phase of TiO_2 (Figure 4(a)). On the other hand, the presence of anatase phase was detected in the sample subjected to annealing at 400°C in air atmosphere (Figure 4(b)). It can be seen that the diffraction peaks of the entire samples are ascribed to the TiO_2 with anatase phase [JCPDS no. 21-1272]. The diffraction peaks allocated at 25.37°, 38.67°, 48.21°, 54.10°, and 55.26° are corresponding to (101), (112), (200), (105), and (211) crystal planes for the anatase phase, respectively.

3.5. Photoelectrochemical Response of the TiO_2 Nanotube Arrays. In order to evaluate the effect of surface area and crystallization of TiO_2 nanotube arrays on its photoelectrochemical response, the as-anodized and annealed samples fabricated from different applied potentials were used as photoelectrodes in the photoelectrochemical process. The photocurrent density-voltage transient was recorded under darkness and illuminated conditions, with a light intensity of approximately 800 W/m^2. Linear sweep potentiometry (LSP) was firstly applied to investigate the photoelectrochemical behaviors of TiO_2 nanotube samples. The corresponding experimental results are presented in Figure 5.

All of the samples exhibited insignificant photocurrents less than 10^{-6} A/cm^2 under dark condition (without illumination). This indicates inactive photoreaction of TiO_2 without generating photoinduced electrons under dark condition. However, the photocurrent density increased under illumination. This situation implies that TiO_2 is a good photoresponse semiconductor for the transfer and decay of photoinduced electrons through the sample [19]. Based on the photocurrent density-voltage (I-V) characteristic, the photocurrent density increased when the voltage was increased from −0.5 V to 1 V under illumination.

A maximum photocurrent density of up to 0.85 mA/cm^2 was observed from the TiO_2 nanotubes fabricated at 30 V; this is relatively high among all of the samples (Figure 5(a)). On the contrary, the as-anodized TiO_2 nanotube (without annealing) had the lowest photocurrent density compared with the annealed TiO_2 nanotube arrays, having a minimum photocurrent density as low as 0.02 mA/cm^2 (Figure 5(f)). The TiO_2 nanotubes fabricated at 20 V, 40 V, 50 V, and 10 V exhibited decreased photocurrent densities, approximately 0.70 mA/cm^2 (Figure 5(b)), 0.50 mA/cm^2 (Figure 5(c)), 0.40 mA/cm^2 (Figure 5(d)), and 0.20 mA/cm^2 (Figure 5(e)), respectively. These results clearly indicate that the differences in crystallization and surface area of the anodic samples influence the photoelectrochemical performance of TiO_2 nanotube.

In Figure 5, the TiO_2 nanotubes were amorphous in the as-anodized condition, which showed poor photocurrent density. However, the photocurrent density was found to increase for annealed TiO_2 nanotube arrays. Transformation of amorphous structure into crystalline phase was observed after annealing at 400°C in air atmosphere. The increase in photocurrent density is likely attributed to the higher photogenerated electron/hole pairs caused by higher content of anatase phase, whereas the presence of amorphous phase reduces the content of electron/hole pairs due to the existence of more recombination centers in amorphous phase [29].

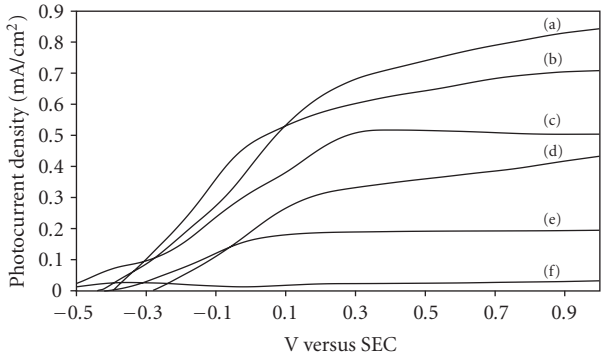

Figure 5: The I-V characteristics of TiO_2 nanotubes with different applied potentials, (a) 30 V, (b) 20 V, (c) 40 V, (d) 50 V, (e) 10 V, and (f) as-anodized sample.

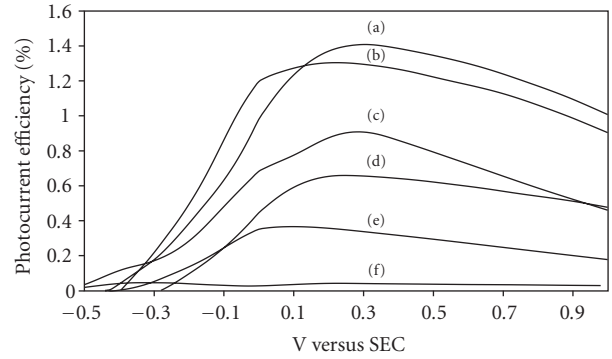

Figure 6: The corresponding photoconversion efficiencies of TiO_2 nanotubes with different anodization potentials, (a) 30 V, (b) 20 V, (c) 40 V, (d) 50 V, (e) 10 V, and (f) as-anodized sample.

The photocurrent density-voltage (I-V) characteristic shows that the higher photocurrent densities of the higher aspect ratio TiO_2 nanotube arrays are strongly dependent upon the availability of larger active surface area for photoelectrochemical reaction. Larger active surface area have better photon absorption as more photoinduced electrons have been effectively transported from TiO_2 nanotube photoanode to counterelectrode through the external circuit under illumination. In addition, photocurrent density can be enhanced by improving the uniformity of the nanotube's size due to the effectively triggered interfacial electron shift, which eventually leads to a more significant promotion of photocurrent [19, 30]. The highly uniform morphology of TiO_2 nanotube arrays provides a high degree of electron mobility along the tube axis. This is because the grains of uniform TiO_2 nanotubes are stretched in the tube growth direction, thus, results in better charge transfer properties compared to nonuniform TiO_2 nanoporous structure.

To estimate the quantitative correlation of light absorption to the different surface area and crystallization of the TiO_2 nanotubes, the photoconversion efficiency (η) of light-to-hydrogen energy was measured (Figure 6) and calculated based on the following equation:

$$\eta\ (\%) = \left[\frac{(\text{total power output} - \text{electrical power output})}{\text{light power input}}\right] \times 100\% = j_p\left[\frac{\left(E^0_{\text{rev}} - \left|E_{\text{app}}\right|\right)}{I_o}\right] \times 100, \quad (3)$$

where j_p is the photocurrent density (mA/cm^2), $j_pE^0_{\text{rev}}$ is the total power output; $j_p|E_{\text{app}}|$ is the electrical power input, I_o is the power density of the incident light (mW/cm^2), E^0_{rev} is the standard reversible potential (1.23 V/SHE), $E_{\text{app}} = E_{\text{mean}} - E_{\text{aoc}}$, E_{mean} is the electrode potential (versus SCE) of the working electrode where the photocurrent was measured under illumination, and E_{aoc} is the potential (versus SCE) of the working electrode at open circuit condition.

Based on the photoconversion efficiency curve shown in Figure 6, the highest visible spectrum efficiency (about 1.4%) was obtained from the nanotube arrays fabricated at 30 V. The decrease in photocurrent efficiency was as follows: 1.30%, 0.90%, 0.65%, 0.38%, and 0.05%, which correspond to the anodic samples fabricated at 20 V, 40 V, 50 V, 10 V, and as-anodized TiO_2 nanotube arrays, respectively. The results clearly indicate that the photoelectrochemical properties are dependent on the crystal structure, surface morphology, and surface area of the nanotubular structure. The increase in number of charge carrier plays an important role on improving the efficiency of the water-splitting process.

4. Conclusion

The effect of applied potential on the surface morphology of TiO_2 nanotube arrays formed in glycerol electrolyte containing 0.5 wt% of NH_4F was investigated. TiO_2 nanotubes having a tube's length of approximately 1 μm and a uniform diameter of 85 nm have been successfully synthesized by anodization of Ti at 30 V. At lower applied potential, the Ti surface consisted of oxide layer with random pits whereas, at higher applied potential, irregular structure was formed as the balance between the chemical dissolution and electric field dissolution, and oxidation process was interrupted. The higher aspect ratio of TiO_2 nanotubes arrays produced at 30 V shows higher photocurrent response among all of the samples. It can be concluded that the effective surface area and crystallization of TiO_2 nanotube arrays are important factors influencing the efficiency of photoelectrochemical performance.

Acknowledgment

The authors would like to thank Universiti Sains Malaysia for sponsoring this work under RU Grant 814075, Fellowship USM, and Research University Postgraduate Research Grant Scheme (Grant no. 80430146).

References

[1] A. Ghicov and P. Schmuki, "Self-ordering electrochemistry: a review on growth and functionality of TiO_2 nanotubes and other self-aligned MOx structures," *Chemical Communications*, no. 20, pp. 2791–2808, 2009.

[2] C. A. Grimes, "Synthesis and application of highly ordered arrays of TiO_2 nanotubes," *Journal of Materials Chemistry*, vol. 17, no. 15, pp. 1451–1457, 2007.

[3] J. Wan, X. Yan, J. Ding, M. Wang, and K. Hu, "Self-organized highly ordered TiO_2 nanotubes in organic aqueous system," *Materials Characterization*, vol. 60, no. 12, pp. 1534–1540, 2009.

[4] J. F. Chen, J. Lin, and X. F. Chen, "Self-assembled TiO_2 nanotube arrays with U-shaped profile by controlling anodization temperature," *Journal of Nanomaterials*, vol. 2010, Article ID 753253, 4 pages, 2010.

[5] M. Kitano, M. Matsuoka, M. Ueshima, and M. Anpo, "Recent developments in titanium oxide-based photocatalysts," *Applied Catalysis A*, vol. 325, no. 1, pp. 1–14, 2007.

[6] X. Quan, S. Yang, X. Ruan, and H. Zhao, "Preparation of titania nanotubes and their environmental applications as electrode," *Environmental Science & Technology*, vol. 39, no. 10, pp. 3770–3775, 2005.

[7] D. Wang, Y. Liu, B. Yu, F. Zhou, and W. Liu, "TiO_2 nanotubes with tunable morphology, diameter, and length: synthesis and photo-electrical/catalytic performance," *Chemistry of Materials*, vol. 21, no. 7, pp. 1198–1206, 2009.

[8] K. S. Raja, M. Misra, and K. Paramguru, "Formation of self-ordered nano-tubular structure of anodic oxide layer on titanium," *Electrochimica Acta*, vol. 51, no. 1, pp. 154–165, 2005.

[9] M. Paulose, H. E. Prakasam, O. K. Varghese et al., "TiO_2 nanotube arrays of 1000 μm length by anodization of titanium foil: phenol red diffusion," *The Journal of Physical Chemistry C*, vol. 111, no. 41, pp. 14992–14997, 2007.

[10] S. Y. Ok, K. K. Cho, K. W. Kim, and K. S. Ryu, "Structure and dye-sensitized solar cell application of TiO_2 nanotube arrays fabricated by the anodic oxidation method," *Physica Scripta*, vol. T139, article 014052, 2010.

[11] S. Li, G. Zhang, D. Guo, L. Yu, and W. Zhang, "Anodization fabrication of highly ordered TiO_2 nanotubes," *The Journal of Physical Chemistry C*, vol. 113, no. 29, pp. 12759–12765, 2009.

[12] D. Gong, C. A. Grimes, O. K. Varghese et al., "Titanium oxide nanotube arrays prepared by anodic oxidation," *Journal of Materials Research*, vol. 16, no. 12, pp. 3331–3334, 2001.

[13] A. Fujishima, X. Zhang, and D. A. Tryk, "TiO_2 photocatalysis and related surface phenomena," *Surface Science Reports*, vol. 63, no. 12, pp. 515–582, 2008.

[14] M. Ni, M. K. H. Leung, D. Y. C. Leung, and K. Sumathy, "A review and recent developments in photocatalytic water-splitting using TiO_2 for hydrogen production," *Renewable and Sustainable Energy Reviews*, vol. 11, no. 3, pp. 401–425, 2007.

[15] C. A. Grimes, O. K. Varghese, and S. Ranjan, *Light, Water, Hydrogen: The Solar Generation of Hydrogen by Water Photoelectrolysis*, Springer, New York, NY, USA, 2008.

[16] Z. Liu, B. Pesic, K. S. Raja, R. R. Rangaraju, and M. Misra, "Hydrogen generation under sunlight by self ordered TiO_2 nanotube arrays," *International Journal of Hydrogen Energy*, vol. 34, no. 8, pp. 3250–3257, 2009.

[17] A. Fujishima and K. Honda, "Electrochemical photolysis of water at a semiconductor electrode," *Nature*, vol. 238, no. 5358, pp. 37–38, 1972.

[18] G. K. Mor, K. Shankar, O. K. Varghese, and C. A. Grimes, "Photoelectrochemical properties of titania nanotubes," *Journal of Materials Research*, vol. 19, no. 10, pp. 2989–2996, 2004.

[19] Y. Xie, L. Zhou, and J. Lu, "Photoelectrochemical behavior of titania nanotube array grown on nanocrystalline titanium," *Journal of Materials Science*, vol. 44, no. 11, pp. 2907–2915, 2009.

[20] Z. Zhang, M. F. Hossain, and T. Takahashi, "Photoelectrochemical water splitting on highly smooth and ordered TiO_2 nanotube arrays for hydrogen generation," *International Journal of Hydrogen Energy*, vol. 35, no. 16, pp. 8528–8535, 2010.

[21] W. Zhu, X. Liu, H. Liu, D. Tong, J. Yang, and J. Peng, "An efficient approach to control the morphology and the adhesion properties of anodized TiO_2 nanotube arrays for improved photoconversion efficiency," *Electrochimica Acta*, vol. 56, no. 6, pp. 2618–2626, 2011.

[22] R. L. D. Whitby, S. F. A. Acquah, R. Z. Ma, and Y. Q. Zhu, "1D nanomaterials," *Journal of Nanomaterials*, vol. 2010, Article ID 597851, 3 pages, 2010.

[23] W. J. Lee, M. Alhoshan, and W. H. Smyrl, "Titanium dioxide nanotube arrays fabricated by anodizing processes: electrochemical properties," *Journal of the Electrochemical Society*, vol. 153, no. 11, pp. B499–B505, 2006.

[24] K. Yu and J. Chen, "Enhancing solar cell efficiencies through 1-D nanostructures," *Nanoscale Research Letters*, vol. 4, no. 1, pp. 1–10, 2009.

[25] G. K. Mor, O. K. Varghese, M. Paulose, N. Mukherjee, and C. A. Grimes, "Fabrication of tapered, conical-shaped titania nanotubes," *Journal of Materials Research*, vol. 18, no. 11, pp. 2588–2593, 2003.

[26] A. Jaroenworaluck, D. Regonini, C. R. Bowen, R. Stevens, and D. Allsopp, "Macro, micro and nanostructure of TiO_2 anodised films prepared in a fluorine-containing electrolyte," *Journal of Materials Science*, vol. 42, no. 16, pp. 6729–6734, 2007.

[27] G. K. Mor, O. K. Varghese, M. Paulose, and C. A. Grimes, "Transparent highly ordered TiO_2 nanotube arrays via anodization of titanium thin films," *Advanced Functional Materials*, vol. 15, no. 8, pp. 1291–1296, 2005.

[28] S. Yoriya, M. Paulose, O. K. Varghese, G. K. Mor, and C. A. Grimes, "Fabrication of vertically oriented TiO2 nanotube arrays using dimethyl sulfoxide electrolytes," *Journal of Physical Chemistry C*, vol. 111, no. 37, pp. 13770–13776, 2007.

[29] V. K. Mahajan, M. Misra, K. S. Raja, and S. K. Mohapatra, "Self-organized TiO_2 nanotubular arrays for photoelectrochemical hydrogen generation: effect of crystallization and defect structures," *Journal of Physics D*, vol. 41, no. 12, Article ID 125307, 2008.

[30] Y. B. Liu, J. H. Li, B. X. Zhou et al., "Comparison of photoelectrochemical properties of TiO_2-nanotube- array photoanode prepared by anodization in different electrolyte," *Environmental Chemistry Letters*, vol. 7, no. 4, pp. 363–368, 2009.